Z.H. Chen, W. Wang, D. Chen* and W.J. Xia

Microstructures and Creep Properties of Mg-2.5Zn-*x*Ce (*x* = 4, 6 and 8 mass%) Alloys

Abstract: The effect of 4, 6 and 8 (mass%) Ce additions on the microstructure and creep resistance of the Mg-2.5Zn alloy was investigated by tensile creep test in the temperature of 200 °C, 225 °C with the tensile stress of 60 MPa and tensile test in room temperature. The microstructure and phase composition of these alloys were analyzed by optical microscopy (OM), scanning electron microscopy (SEM), energy dispersive X-ray spectroscopy (EDS) and X-ray diffractometry (XRD). The results showed that the grain sizes of Mg-2.5Zn-*x*Ce alloys were decreased and the creep strength of the base alloy was remarkably improved by increasing Ce addition. This were attributed to the formation of $Mg_{12}Ce$, Mg_2Ce and $(Mg,Zn)_{12}Ce$ compounds that morphology remains relatively stable at moderately elevated temperature which strengthen both matrix and grain boundaries during creep deformation.

Keywords: Mg-Zn-Ce alloy, tensile creep, Ce addition, $(Mg,Zn)_{12}Ce$ phase

PACS® (2010). 62.20.Hg

DOI 10.1515/htmp-2014-0050
Received March 15, 2014; accepted May 5, 2014;
published online June 24, 2014

1 Introduction

Magnesium alloys are promising light structural materials because of their excellent properties such as high specific strength and high specific stiffness. The use of Mg alloys is expanding, particularly in the automobile and consumer electronics industries [1, 2]. However, one of the limitations of magnesium alloys for structural applications is their low creep resistant properties at elevated temperatures [3]. Thus enhancing creep properties of magnesium alloys becomes very important.This can be achieved by using various alloying elements, which can form thermally stable second-phase constituents in the as-cast condition [4]. From the results of the previous studies [5–7], rare earth (RE) elements, with certain special characteristics, are well known for their positive effects in Mg alloys. The use of rare earths enables both solid solution hardening and precipitation hardening, and the intermetallic phases exhibit little diffusivity and a good coherence to the matrix [8]. Currently the Mg-RE system is the only magnesium alloys that can offer adequate creep resistance for application at temperatures that above 200 °C [9]. Not only the volume fraction but also the arrangement, the orientation relationship and aspect ratio of the precipitates of RE affect the mechanical and creep properties [10–16]. Cerium is a major component of misch-metal and thus is considered as the most important part in these industrially used rare earth elements.It has been reported that addition of Ce affects excellent age hardening behavior for the Mg-1.5Zn-0.2Ce (mass%) alloy [17]. In addition, Zn in low quantities has also proven to aid tensile and creep strength [18].

Many research have been proposed effects of low levels of Ce in the Mg alloys [19–21]. However, several experimental studies have carried out on the high levels of Ce. In this paper, a selected amount of Ce, namely 4, 6 and 8 (mass%), was added into the Mg-2.5Zn alloy. The microstructure and creep properties of Mg-2.5Zn alloy at elevated-temperature were studied, aiming at clarifying the factors that affect the microscopic morphology and the creep performance of alloys.

2 Experimental

2.1 Materials and processing

The materials used in the experiments were commercially pure magnesium (99.95 mass%), pure Zinc (99.90 mass%) and Mg-30 (mass%) Ce master alloy. Mg-2.5Ce-*x*Ce (*x* = 4, 6, 8 mass%) alloys are produced by gravity casting. The magnesium alloys were prepared in a steel crucible in an electrical resistance furnace. The mixtures were under cover flux (main compositions: 38–46% $MgCl_2$,

***Corresponding author: D. Chen:** College of Materials Science and Engineering, Hunan University, Changsha 410082, China.
E-mail: ma97chen@hotmail.com
Z.H. Chen, W. Wang, W.J. Xia: College of Materials Science and Engineering, Hunan University, Changsha 410082, China

Table 1: Chemical compositions (mass%) of the Mg-2.5Zn-*x*Ce (*x* = 4, 6, 8) alloys

Alloys (mass%)	Ce	Zn	Fe	Mn	Mg
Mg-2.5Zn-4Ce (#1)	4.11	2.52	<0.02	<0.01	bal.
Mg-2.5Zn-6Ce (#2)	6.04	2.49	<0.02	<0.01	bal.
Mg-2.5Zn-8Ce (#3)	7.94	2.46	<0.02	<0.01	bal.

32–40% KCl, 5–8% $BaCl_2$, 3–5% CaF_2, and 8% NaCl+$CaCl_2$) to protect molten magnesium from oxidation during melting and the melton temperature was about 760 °C. The melts were cast into a steel mould. All kinds of Mg-Zn-Ce alloys with nominal compositions of 2.5 mass% Zn and 4, 6, 8 mass% Ce were used as-received specimens by wire-electrode cutting. The cast slabs were cut into slices of 84 mm in length, 16 mm in width and 2 mm in thickness using an electrodischarge wire-cut machine for the tensile creep tests and cut into slices of 15 mm in length, 3.2 mm in width and 1.8 mm in thickness for tensile tests. The chemical compositions of the Mg-2.5Zn-*x*Ce (*x* = 4, 6, 8) alloys are listed in Table 1. The as-cast microstructure and the evolution of microstructure after creep was measured with optical microscope (OM), as well as with scanning electron microscope (SEM). The samples for OM and SEM were polished and etched by using an etchant consisting of 1 mL HNO_3 and 20 mL ethylic acid and 30 mL water. Analysis of phase was investigated by X-ray diffraction (XRD). The chemical compositions of the analyzed phases of the alloys were measures by energy dispersive X-ray spectroscopy (EDS) in the scanning electron microscope.

2.2 Tensile creep tests

Tensile creep tests were performed on the type of GWT304 high-temperature creep test machine to carry out constant-load tensile creep tests in the air atmosphere. The specimen was located between two loading bars. The tests were performed in the temperatures of 200 °C and 225 °C and under a stress of 60 MPa for dwell times of 70 h. An electronic temperature control three-zone split furnace was used and the temperature with an accuracy of ±2 °C during the test. The test to control the load with an accuracy of ±2N. The data were acquired by an computer.

2.3 Mechanical testing

Room temperature tension experiments were performed at a strain rate of 10^{-5} s^{-1} using an Instron 3369 mechanical testing machine. The ultimate tensile stress, the tensile strength (MPa), and the yield strength (MPa) were recorded for each test. Perpare three specimens for per alloy to tensile tested and the reported properties were averaged. The experiments were performed under constant load and the temperature–strain–time data were collected by computer. Selected specimens were taken to failure.

3 Results and discussion

3.1 Microstructural observations

The optical microstructures of the cast Mg-2.5Zn-*x*Ce alloys are shown in Fig. 1. As can be seen, it is evident that each alloy presents a typical dendritic cast structure with interphases at interdendritic regions. It's noticeable that the volume fraction of which increases with increase of Ce addition in the alloys, and the RE elements are concentrated in the interdendritic boundary areas during solidification. Besides, along with the increase of Ce additions the continuity of interdendritic network becomes strong and the eutectics are thickened. From Fig. 1, we can see that the average grain sizes of the three alloys were about 200 μm, 140 μm and 70 μm, respectively. Apparently, the #3 and #2 alloys exhibited smaller grain sizes than the #1 alloys. This suggests that the RE additions have effectively refined the grain structures of base alloy.

Mechanisms of grain refinement are linked to the path of phase formation and the solidification closely [22]. Magnesium matrix solidified firstly with temperature reduction, because the solid solubility of Ce in the Mg matrix is very low. So the Mg-Ce intermetallic compound is very difficult to become a heterogeneous nuclei of *α*-Mg. The grain of *α*-Mg matrix growth during solidification, push the rare earth phase to the solid-liquid interface constantly, then solute redistribution was formed. Rare earth phase enriched in the front of solid/liquid interface in the solidification process then caused constitutional supercooling, the supercooled region formed with new nuclear and the fine equiaxed grains were formed [23]. The undercooling region increased with the increase of the content of rare earth. The volume fraction of equiaxed second phase increased, the formation of network structure separated the magnesium matrix then the refined the grain of alloys, objectively.

Representative SEM micrographs of the alloys are shown in Fig. 2. It is evident that the second phases are substantial enrichment at the grain boundaries. EDS (Fig. 3) indicated that the intermetallic phase contained Ce, Mg

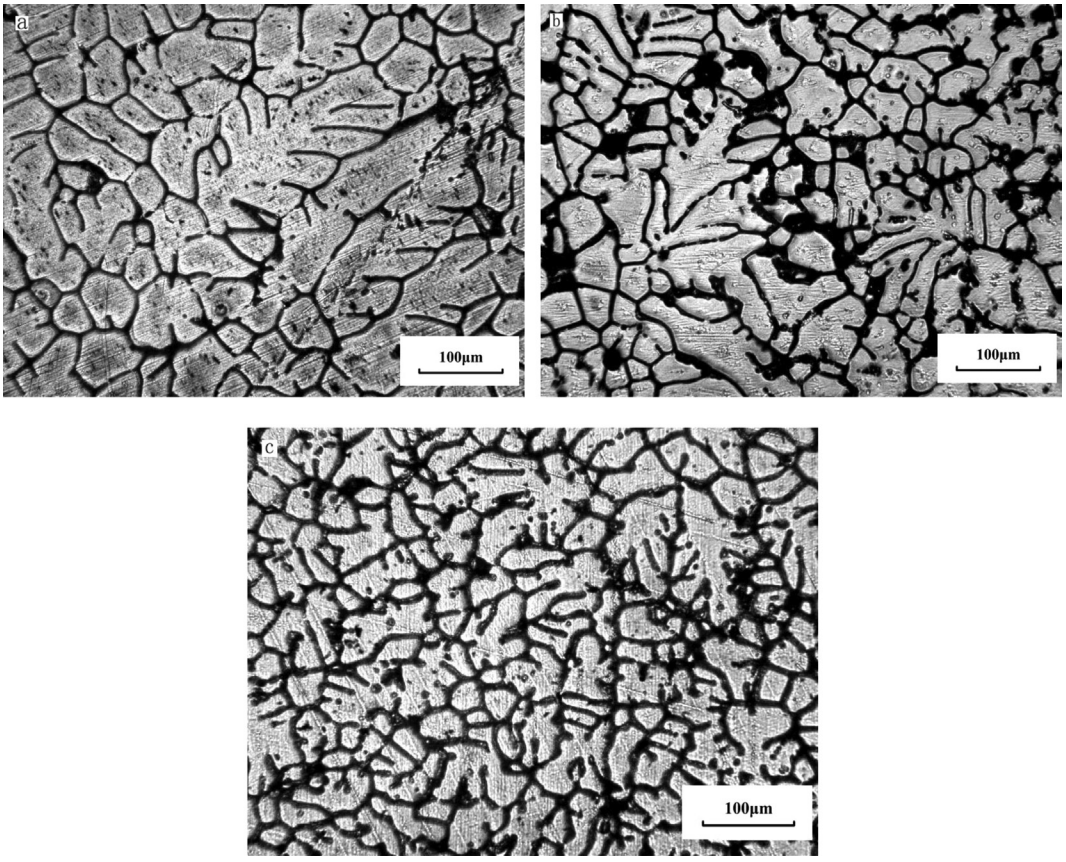

Fig. 1: Optical micrographs of cast Mg alloys: (a) Mg-2.5Zn-4Ce, (b) Mg-2.5Zn-6Ce, (c) Mg-2.5Zn-8Ce

and Zn. Matrix contains vast majority of Mg and only a small amount of Zn. Table 2 shows Chemical compositions (at%) of matrix and second phase of the Mg-2.5Zn-*x*Ce ($x = 4$, 6, 8) alloys. Fig. 4 shows the XRD spectrum of Mg-2.5Zn-*x*Ce (as-cast). Clearly, from the Fig. 2. We can see that the phase composition of the three cast alloys don't change much. All three alloys contain α-Mg phase, $Mg_{12}Ce$ phase and a small amount of Mg_2Ce phase. In addition, with the increase of Ce content, the diffraction peak of the second phase become more and more obvious. However, no binary phase of Mg-Zn in the three alloys was found by the XRD. Parts of Zn are located in the $Mg_{12}Ce$ phase due to the strong attraction effects of Ce element. Therefore, the $Mg_{12}Ce$ phase in the Zn-containing alloy probably exists in the form of the $(Mg,Zn)_{12}Ce$ intermetallic compound. This shows that the second phase in the interdendritic regions is not merely Mg-Ce and Mg-Zn binary phase, with Ce and Zn, Mg forming a relatively high melting point (470~500 °C) of Mg-Zn-Ce phase (T-phase), can improve the thermal stability of the alloy greatly. And #3 samples (Fig. 2c) contain the highest of Ce, which can form more $Mg_{12}Ce$, Mg_2Ce phase and T phase, and further improves the creep resistance properties of alloys.

3.2 Creep behavior and mechanical properties

The creep curves of three kinds of samples under 60 MPa for the temperature of 200 °C (Fig. 5a) and 225 °C (Fig. 5b) are shown in Fig. 5 and the details of these curves are summarized in Table 3. Fig. 5a shows that creep time of the three kinds of alloys are more than 70 h, but the tertiary creep stage did not appear. With the increase content of RE, the creep properties of the alloy in elevated temperature are improved. There is little difference in steady-state creep rate between #2 samples and #3, seen in Table 2, which is 9.8×10^{-8} s^{-1} and 1×10^{-8} s^{-1}, respectively. They are at the same level. The reason may be that the testing temperature and stress are low, the creep life of sample is long, while the figure only shows second stages of creep. But the steady creep rate of #1 sample was 3.2×10^{-7} s^{-1}, which is higher than that of #2 and #3 samples significantly. Fig. 5b shows the creep curves of Mg-2.5Zn-*x*Ce, in the temperature of 225 °C. Compared with that of 220 °C, the creep resistance decreased, but the overall trend still increased with the increase of RE content and creep resistance of alloys. The creep time of sample #1 was only

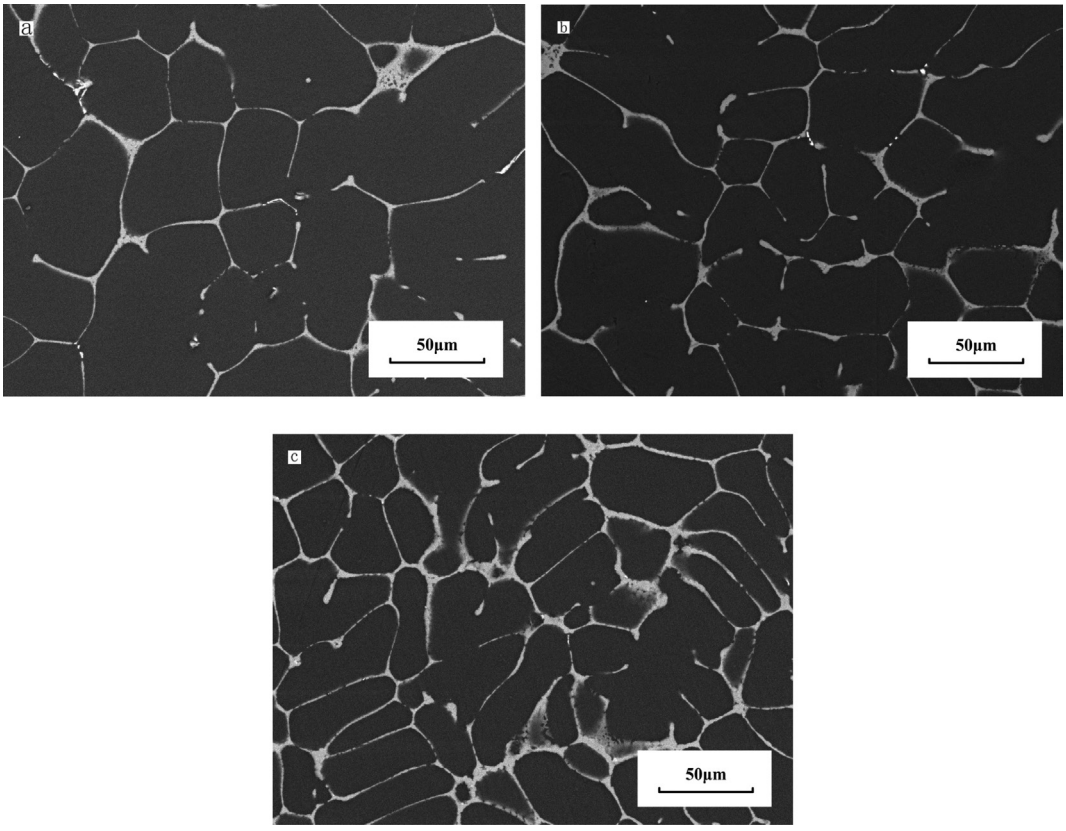

Fig. 2: SEM micrographs of cast Mg-2.5Zn-*x*Ce: (a) 4Ce, (b) 6Ce, (c) 8Ce

18.2 h, then the sample was fractured. And sample #2 shows a typical creep curves with three stages, the creep time was 30.16 h. The creep resistance of sample #3 is the best in all three kinds of alloys, but did not appear the third stage, the creep time was more than 70 h.

Fig. 6 shows the change of the second phase of Mg-2.5Zn-4Ce before (a) and after (b) the creep test in the temperature of 200 °C. Fig. 6a shows that second phase in the interdendritic grain boundary was continuous and complete, compared with Fig. 6b a lot of crack were generated in the second phase in the interdendritic boundary areas of alloy after creep.

As known, for the pure metal and solid solution alloys, the size of grain has a significant effect on the creep performance. But for the existence of second phase particles on grain boundary, this effect tends to reduce [24]. According to scanning electron microscopy picture, the second phase of RE distributed in grain boundaries, especially enriched in triangle grain boundary. The structure of secondary phase which not continuous or semi continuous changed into a continuous network structure with the increase of RE content. The increase of RE content could produce more secondary phase. According to the analysis of XRD (Fig. 4) and EDS (Fig. 3) the second phase mainly consists of $Mg_{12}Ce$ and a small amount of Mg_2Ce phase. Some scholars confirmed that the hardness and elastic modulus of the eutectic $Mg_{12}Ce$ between grain boundary are indeed higher than α-Mg matrix by nano-indentation experiments. And the average indentation hardness increased with the increasing of Ce content [25]. The establishment of the skeleton in magnesium alloy by the strengthening phase composition has very important significance to improve the elevated temperature creep resistance of magnesium alloy [26, 27]. The addition of Ce element to the Mg-Zn alloy formed $Mg_{12}Ce$ and $(Mg,Zn)_{12}Ce$ phase, and then the second phase formed a three-dimensional continuous network structure between the grains. The structure can securely wrap grains up, so softening or breaking of the structure need for higher temperatures and greater stress. Micro-fracture accumulated to a certain extent, produce deformation macroscopically. When the network of subsequent second phase was broken, it would produce a lot of particles of second phase, these particles, which be pinned on the grain boundary, would produce to impede grain boundary sliding. Due to the high softening temperature (470~500 °C) of second phase, structure is relatively stable. As the stress increases, the large amount of second

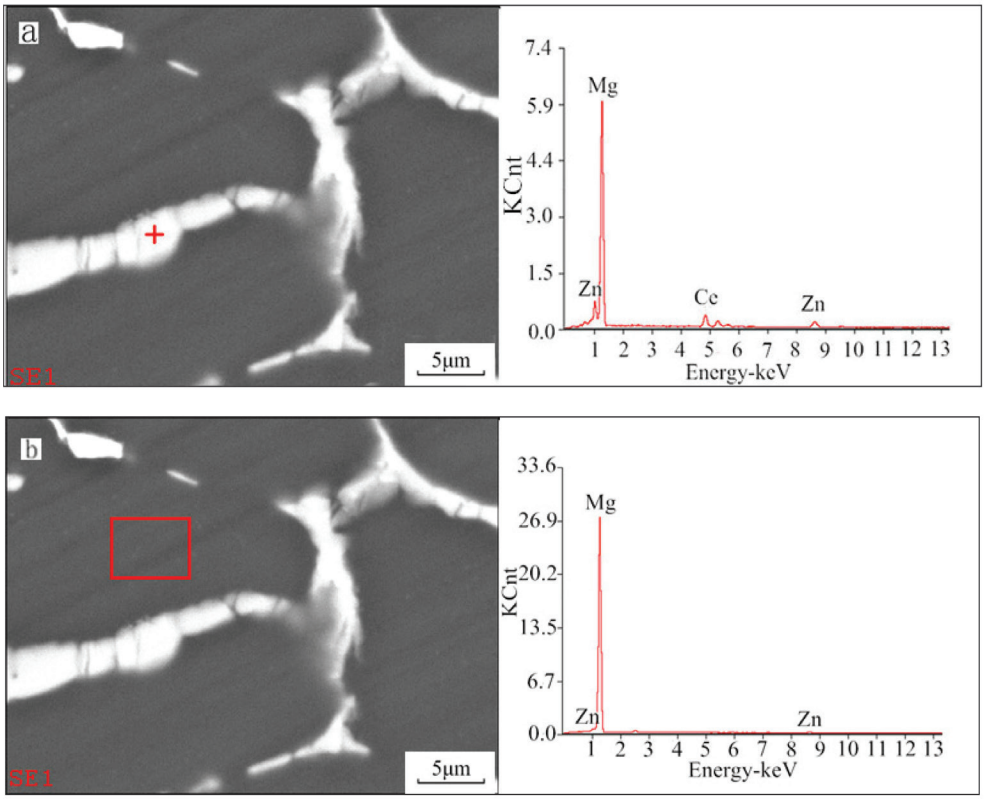

Fig. 3: SEM and EDS analysis of Mg-2.5Zn illustrating (a) a grain boundary particle (light contrast) enriched in Ce, Mg, and Zn, (b) matrix composition enriched in Mg and Zn

Table 2: Chemical compositions (at%) of matrix and second phase of the Mg-2.5Zn-*x*Ce (*x* = 4, 6, 8) alloys

Alloy		Mg (at%)	Zn (at%)	Ce (at%)
Mg-2.5Zn-4Ce	Matrix	99.32	0.68	–
	Second phase	87.79	7.03	5.18
Mg-2.5Zn-6Ce	Matrix	99.25	0.75	
	Second phase	87.77	6.80	5.43
Mg-2.5Zn-8Ce	Matrix	99.65	0.35	
	Second phase	87.80	6.94	5.26

phase can effectively absorb the deformation energy. When the Ce content is lower, the grain size is larger, which means the skeleton structure of the second phase is not denser than the alloy of higher Ce content. And the thickness of the second phase along the grain boundary is relatively weak compared with the second phase of high content of RE. The second phase is less in unit area where under pressure compared to the dense network structure phase broken easily. But under the condition of high Ce, the greater the amount of second phases on the stress-bearing surface is, the more stress to bear, as shown in Fig. 7.

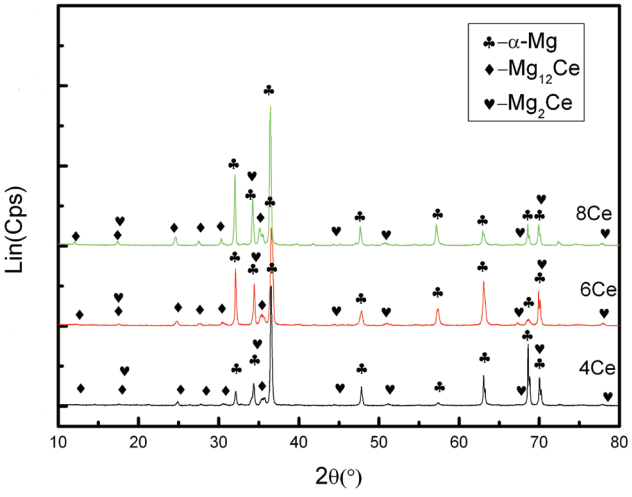

Fig. 4: XRD spectrum of Mg-2.5Zn-*x*Ce (as-cast)

Typical tensile stress-strain curves of the investigated alloys at room temperature are presented in Fig. 8. It can be observed that after a linear elastic behavior the curves deviate from linearity before reaching a maximum point to the tensile strength. Table 4 shows that the tensile strength (MPa), and the yield strength (MPa) of the three

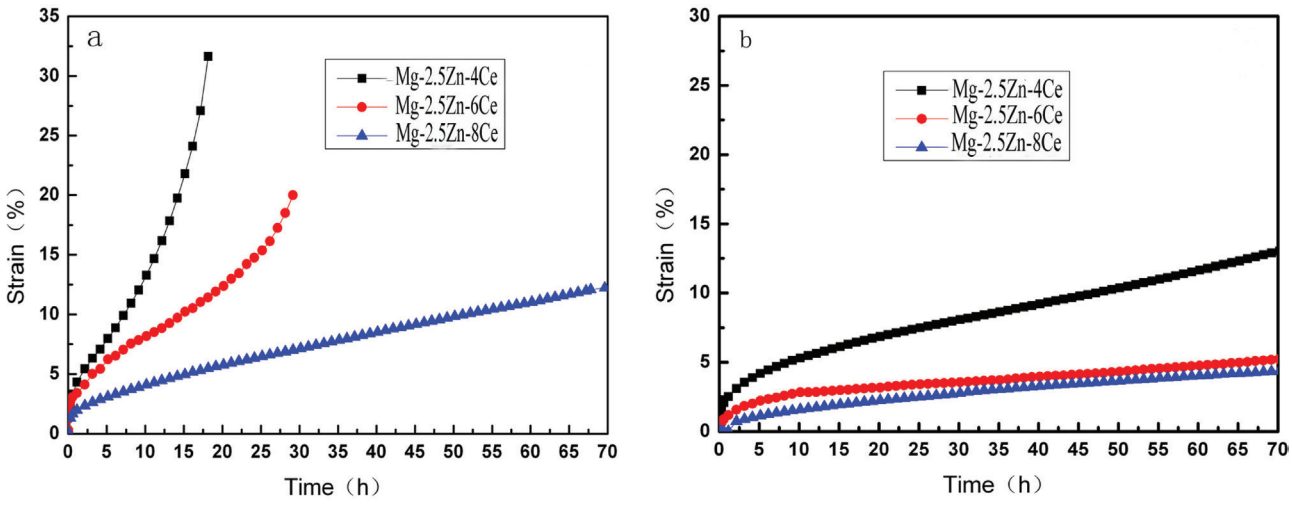

Fig. 5: Creep curves of Mg-2.5Zn-*x*Ce: (a) 200 °C, 60 MPa, 70 h, (b) 225 °C, 60 MPa, 70 h

Table 3: The steady state creep rate, creep time and elongation of the three groups of samples

Alloys (mass%)	Stress (MPa)	T (°C)	Steady state creep rate (s^{-1})	Time (h)
Mg-2.5Zn-4Ce	60	200	3.2×10^{-7}	>70
	60	225	4.9×10^{-6}	18.2
Mg-2.5Zn-6Ce	60	200	9.8×10^{-8}	>70
	60	225	1.2×10^{-6}	30.2
Mg-2.5Zn-8Ce	60	200	1.0×10^{-8}	>70
	60	225	3.7×10^{-7}	>70

groups of samples at room temperature. As can be seen, #2 alloy exhibits maximum yield strength and tensile strength which contains 6Ce. These are 105.48 MPa and 156.65 MPa, respectively. #1 alloy exhibits minimum yield strength and tensile strength which contains 4Ce. These are 92.95 MPa and 131.76 MPa, respectively. The yield strength and tensile strength of #3 alloy lower than #2 alloy but greater than #1 alloy. It is seen that the addition of Ce clearly improves the tensile strength, which increases gradually with Ce addition up to 6 mass%, but further increasing Ce contents leads to reduction of tensile strength. According to Fig. 6, the specimens of 6Ce showed the best mechanical properties.

It is well known that the RE elements have poor solid solubility in magnesium [28], which suggests RE additions have a limit for solid–solution strengthening. Therefore, the following two factors of the improvement of tensile properties should be considered: (a) The coarse eutectic microstructure located at grain boundaries is refined due to the increasing content of RE, and the refined eutectic benefits the tensile strength; (b) dispersive second phase particles formed after Ce additions can restrain dislocation movement, which favors tensile strength [29]. However, at higher Ce (8 mass%) additions, more formation

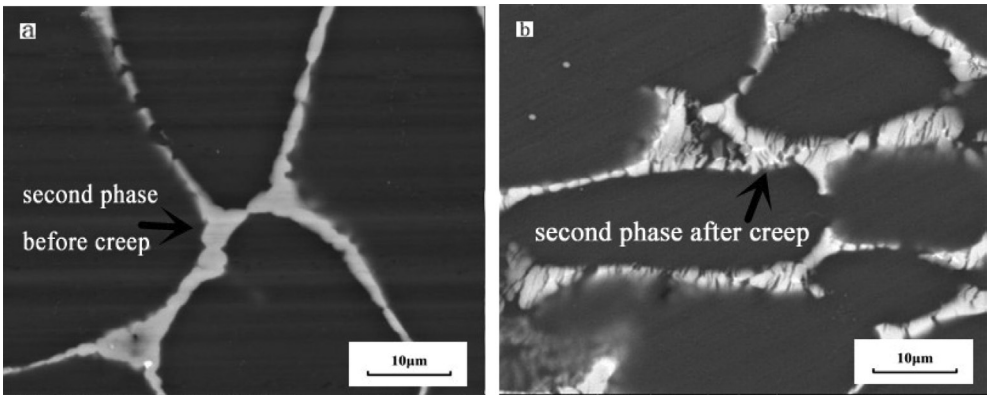

Fig. 6: The change of the second phase before (a) and after (b) the creep test (Mg-2.5Zn-4Ce, 200 °C, 60 MPa)

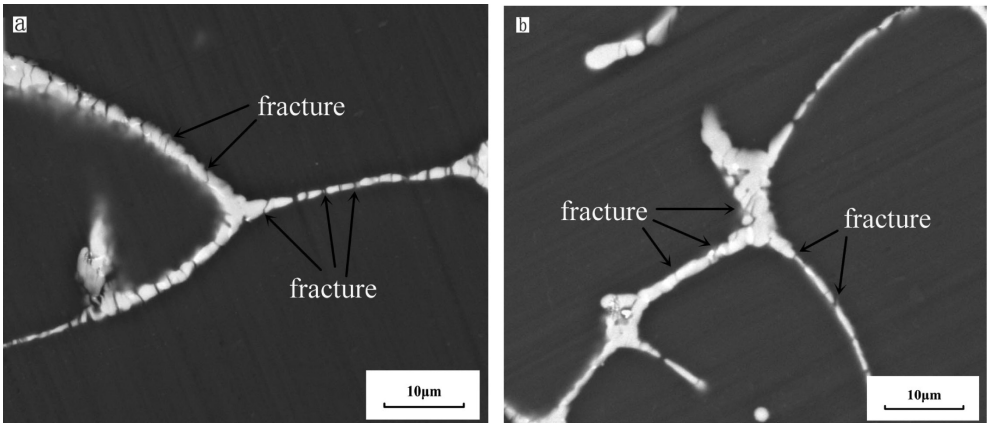

Fig. 7: The difference of the fractured second phase after the creep test (200 °C, 60 MPa): (a) Mg-2.5Zn-8Ce, (b) Mg-2.5Zn-4Ce

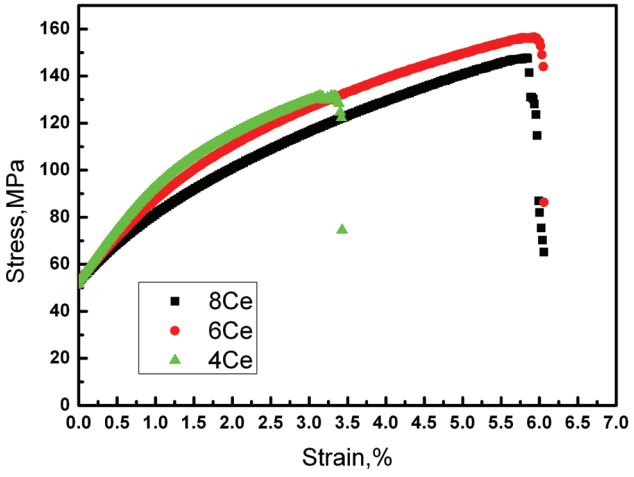

Fig. 8: Representative tensile stress vs. strain curves for the studied alloys at room temperature

of coarse particles in, incoherent with matrix, which are fragmented under the load, usually leads to poor mechanical properties.

4 Conclusions

The effect of Ce additions on the microstructure and creep properties of Mg-2.5Zn-*x*Ce ($x = 4$, 6 and 8, mass%) alloys was investigated. The conclusions are summarized as follows:

1. The addition of Ce refined the as-cast microstructure. When the Ce content increases from 4 wt% to 8 wt%, the grain size decreased from about 200 μm to 70 μm. The main mechanism of RE element refining magnesium alloys is that solute redistribution during solidification caused by solid-liquid interface undercooling increases the forefront of ingredients.
2. With the increase of Ce content in the alloy, the creep rate decreases, the number density of eutectic thermally stable $Mg_{12}Ce$, Mg_2Ce and $(Mg,Zn)_{12}Ce$ phase at the grain boundaries increased. Because the network structure of second phase can be formed, so it produced strong impediment for grain boundary sliding. Further, the presence of small amounts of the second phase in the matrix prevents slip dislocations which plays a dispersion strengthened effect. With the increase of rare earth content and the volume fraction of second phase, high temperature creep properties of the alloy increases.
3. The mechanical properties of as-cast alloys increase with Ce addition up to 6 mass%, but decrease with Ce addition up to 8 mass%. The yield strength and tensile strength of which contains 4Ce, 6Ce, 8Ce alloy are 92.95 MPa and 131.76 MPa, 105.48 MPa and 156.65 MPa. These are 96.86 MPa and 147.79 MPa,

Table 4: The tensile strength (MPa) and yield strength (MPa) of the three groups of samples at room temperature

Sample	Thickness (mm)	Width (mm)	Length (mm)	The maximum load (N)	Tensile strength (MPa)	Yield strength (MPa)
Mg-2.5Zn-4Ce	1.80	3.20	15.00	758.92	131.76	92.95
Mg-2.5Zn-6Ce	1.80	3.20	15.00	902.32	156.65	105.48
Mg-2.5Zn-8Ce	1.80	3.20	15.00	851.26	147.79	96.86

respectively. 6Ce alloy showed the best mechanical properties.

Funding: Authors greatly acknowledge the financial support by Hunan Provincial Natural Science Foundation of China (14JJ1013).

References

[1] C.J. Boehlert, K. Knittel, *Mater. Sci. Eng., A*, 417 (2006) 315–321.
[2] Y. Chino, X.S. Huang, K. Suzuki, K. Sassa and M. Mabuchi, *Mater. Sci. Eng., A*, 528 (2010) 566–572.
[3] A. Luo, M.O. Pekguleryuz, *J. Mater. Sci.,* 29 (1994) 5259–5271.
[4] R. Alizadeh, R. Mahmudi, *Mater. Sci. Eng., A*, 527 (2010) 5312–5317.
[5] R.Z. Wu, Y.S. Deng and M.L. Zhang, *J. Mater. Sci.,* 44 (2009) 4132–4139.
[6] M.L. Zhang, R.Z. Wu and T. Wang, *J. Mater. Sci.,* 44 (2009) 1237–1240.
[7] G.H. Su, L. Zhang, L.R. Cheng, Y.B. Liu and Z.Y. Cao, *Trans. Nonferrous Met. Soc. China*, 20 (2010) 383–389.
[8] M.O. Pekgueleryuez and M.M. Avedesian, in: B.L. Mordike and F. Hehmann (eds.), *Magnesium Alloys and Their Applications*. DGM-Informationsges, Oberursel, Germany, (1992), pp. 213–220.
[9] D.H. Stjohn, Q. Ma, M.A. Easton, P. Cao and Z. Hildebrand, *Metall. Mater. Trans. A,* 36A (2005) 1669–1679.
[10] J.F. Nie, *Scr. Mater.,* 48 (2003) 1009–1015.
[11] B. Smola, I. Stulíková, J. Pelcová and B.L. Mordike, *J. Alloys Compd.,* 378 (2004) 196–201.
[12] Q. Peng, J. Wang, Y. Wu, J. Meng and L. Wang, *Mater. Charact.,* 59 (2008) 435–439.
[13] J.F. Nie and B.C. Muddle, *Acta Mater.,* 48 (2000) 1691–1703.
[14] B. Smola, I. Stulíková, F.V. Buch and B.L. Mordike, *Mater. Sci. Eng., A*, 324 (2002) 113–117.
[15] P.J. Apps, H. Karimzadeh, J.F. King and G.W. Lorimer, *Scr. Mater.,* 48 (2003) 1023–1028.
[16] I. Stulíková and B. Smola, *Mater. Charact.,* 61 (2010) 952–958.
[17] Y. Chino, K. Sassa and M. Mabuchi, *Mater. Trans.,* 49 (2008) 1710–1712.
[18] M. Suzuki, T. Kimura, J. Koike and K. Maruyama, *Scr. Mater.,* 48 (2003) 997–1002.
[19] M. Celikin, A.A. Kaya, R. Gauvina and M. Pekguleryuz, *Scr. Mater.,* 66 (2012) 737–740.
[20] S. Amira, D. Dubé, R. Tremblay and E. Ghali, *Mater. Charact.,* 76 (2013) 48–54.
[21] M.B. Yang, T.Z. Guo, C.Y. Qin, and F.S. Pan, *J. Rare Earth,* 30 (2012) 181–188.
[22] S. Golmakaniyoon and R. Mahmudi, *Mater. Sci. Eng., A*, 528 (2011) 1668–1677.
[23] L.B. Wu, X.H. Liu, R.Z. Wu, C.L. Cui, J.H. Zhang and M.L. Zhang, *Trans. Nonferrous Met. Soc. China*, 22 (2012) 779–785.
[24] S.M. Zhu, M.A. Gibson, M.A. Eastona and J.F. Nie, *Scr. Mater.,* 63 (2010) 698–703.
[25] K.C. Park, B.H. Kim, Y.H. Park and I.M. Parke, *Trans. Nonferrous Met. Soc. China*, 20 (2010) 1240–1243.
[26] D. Amberger, P. Eisenlohr and M. Göken, *Acta Mater.,* 60 (2012) 2277–2289.
[27] W. Blum, P. Eisenlohr, X.H. Zeng and K. Milička. *Creep of Mg-alloys*, in: M.O. Pekguleryuz and L.W.F. Mackenzie (eds.), *Magnesium Technology in the Global Age*, Metallurgy and Petroleum, Canadian Institute of Mining, (2006), pp. 633–646.
[28] L.B. Wu, C.L. Cui, R.Z. Wu, J.Q. Li, H.B. Zhan and M.L. Zhang, *Mater. Sci. Eng., A,* 528 (2011) 2174–2179.
[29] S.K. Das and L.A. Davis, *Mater. Sci. Eng., A,* 98 (1988) 1–12.